

Actuator Fault Diagnosis Using High-Order Sliding Mode Differentiator (HOSMD) and Its Application to a Laboratory 3D Crane ^{*}

Weitian Chen, Qing Wu, Esmail Tafazzoli, Mehrdad Saif^{*}

^{*} *Simon Fraser University, Vancouver, BC, Canada (e-mail: weitian, qingw, etafazzo, saif@ensc.sfu.ca).*

Abstract: Actuator fault diagnosis problem is studied for a class of nonlinear systems with relative degrees from the inputs to the outputs higher than one. This type of nonlinear systems include many mechanical systems, and their actuator fault diagnosis problem can be very challenging because of nonlinearities and high relative degrees. In this paper, in order to solve the actuator fault diagnosis problem for the considered nonlinear systems, 2nd-order and 3rd-order sliding mode differentiators are used and actuator fault diagnosis schemes are proposed to achieve fault detection and isolation. Computer simulations are carried out to compare the efficacy of the proposed fault diagnosis schemes on a laboratory 3D Crane model with noisy measurements. The fault diagnosis schemes are further tested through experiments on a laboratory 3D Crane in terms of actuator fault detection and isolation.

1. INTRODUCTION

Nonlinearities and unknown inputs (for example, uncertainties and/or unknown disturbances) present real challenges to model based fault diagnosis. To deal with various types of unknown inputs, one most often used strategy is to remove the effect of the unknown inputs completely by designing fault diagnosis schemes that are invariant to the unknown inputs. Some unknown input observer (UIO) and sliding mode observer (SMO) based schemes adopt this strategy. For example, UIO based schemes can be found in Saif and Guan (1993); Chen et al. (1996); Xiong and Saif (1998), while SMO based ones can be found in Sreedhar et al. (1993); Yang and Saif (1995); Xiong and Saif (2001); Jiang et al. (2004); Floquet et al. (2004); Chen and Saif (2005).

To deal with nonlinearities, several attempts have been made on developing nonlinear fault diagnosis schemes. Nonlinear UIO based schemes can be found in Yang and Saif (1997) for bilinear systems, in Yaz and Azemi (1998); Rajamani and Ganguli (2004); Chen and Saif (2006) for Lipschitz nonlinear systems, and in Seliger and Frank (1991a,b) for a more general class of nonlinear systems. Nonlinear SMO based schemes have been proposed in Sreedhar et al. (1993); Yang and Saif (1995); Xiong and Saif (2001); Jiang et al. (2004); Floquet et al. (2004); Chen and Saif (2005). High-gain observer based nonlinear fault diagnosis scheme was designed in Hammouri et al. (1999). Using a geometric approach, nonlinear fault diagnosis schemes were designed in Persis and Isidori (2001); Join et al. (2005).

Conventional UIOs and SMOs proposed for fault diagnosis often require certain matching conditions. One matching

condition is that the relative degrees from the unknown and/or known inputs to the outputs be one. This requirement can not be satisfied by many mechanical systems. Removing this relative degree limitation of observer based design presents a challenge in fault diagnosis, especially in actuator fault diagnosis. High order sliding mode techniques have been found suitable for dealing with the relative degree difficulty (Levant (2003); Floquet and Barbot (2004); Davila et al. (2005); Msirdi et al. (2006)). Because of this, they are very promising in fault diagnosis of systems with high relative degrees. In Chen and Saif (2006) and also in Chen and Saif (2007a), high order sliding mode differentiators were used in actuator fault diagnosis for uncertain linear systems with arbitrary relative degrees. The use of high order sliding mode differentiators in actuator fault diagnosis was extended to a class of affine nonlinear systems with unknown inputs in Chen and Saif (2007b). Higher sliding mode observers were also used for the purpose of fault diagnosis. In Wu and Saif (2007) and Edwards et al. (2007), 2nd-order and/or 3rd-order sliding mode observers were designed to achieve fault diagnosis for systems with relative degrees of two.

In this paper, the idea of using high order sliding mode differentiators in actuator fault diagnosis is applied to a class of nonlinear systems with relative degrees equal to or higher than two, and actuator fault diagnosis schemes using 2nd-order and 3rd-order sliding mode differentiators are proposed to achieve fault detection and isolation. The purpose of this paper is to test and compare the efficacy of actuator fault diagnosis schemes using high order sliding mode differentiators through intensive computer simulations and experiments on a laboratory 3D Crane.

2. SYSTEM OF INTEREST AND PROBLEM FORMULATION

Consider a class of nonlinear systems described as below

^{*} This research was supported by Natural Sciences and Engineering Research Council (NSERC) of Canada through its *Discovery Grant Program*.

$$\begin{aligned} \dot{q}_1(t) &= q_2(t) \\ \dot{q}_2(t) &= f(q_1(t), q_2(t)) + g(q_1(t), q_2(t))u \\ y(t) &= q_1(t) \end{aligned} \quad (1)$$

where $q_1 \in R^n$ and $x = (q_1^T(t) \ q_2^T(t))^T$ is the system state vector, $y(t)$ and $u(t)$ are the output vector and input vector respectively. Moreover, $f(q_1(t), q_2(t)) = (f_1(q_1(t), q_2(t)) \ \cdots \ f_n(q_1(t), q_2(t)))^T$ is an n -dimensional function vector and $g(q_1(t), q_2(t))$ is a function matrix in $R^{n \times m}$. $u(t) = (u_1(t) \ \cdots \ u_m(t))^T$. In the remaining part of this paper, the dependence on time t will be dropped off for simplicity, for example, $q_1(t)$ and $f(q_1(t), q_2(t))$ will be written as q_1 and $f(q_1, q_2)$, respectively.

- Assumption A1: All the functions in $f(q_1, q_2)$ and $g(q_1, q_2)$ are known.
- Assumption A2: $g(q_1, q_2)$ is of full column rank in the region of interest.

It is easy to see that all the relative degrees from the inputs in u to the outputs in y are equal to or higher than two. If $f(q_1, q_2)$ and $g(q_1, q_2)$ contain general nonlinear functions, nonlinear observer design for (1) is quite challenging if high order sliding mode techniques are not used. Because of this, actuator fault diagnosis for the system is difficult without using high order sliding mode techniques. This is the main motivation for using high order sliding mode differentiators in actuator fault diagnosis.

For system (1), the following problem is formulated.

Actuator Fault Diagnosis Problem:

Under the condition that assumptions A1 and A2 are satisfied, design actuator fault diagnosis schemes for (1) such that they can detect and isolate actuator faults.

3. HIGH ORDER SLIDING MODE DIFFERENTIATORS

As will be seen in the next section, for system (1), if \dot{q}_2 and q_2 were known, actuator fault diagnosis would become an easy task under assumptions A1 and A2. Therefore, the main task of actuator fault diagnosis is to find ways to get \dot{q}_2 and q_2 based on the measurements provided by y . Note that $q_2 = \dot{y}$ and $\dot{q}_2 = \ddot{y}$, obtaining \dot{q}_2 and q_2 is equivalent to obtaining the estimates for the first and second order derivatives of y .

In order to obtain the first and second order derivatives of y , a recently developed high order sliding mode differentiator in Levant (2003) is introduced in the following subsection.

3.1 A high order sliding mode differentiator

Let $f(t) = f_0(t) + n(t)$ be a function on $[0, \infty)$, where $f_0(t)$ is an unknown base function with the n -th derivatives having a Lipschitz constant L , and $n(t)$ is a bounded Lebesgue-measurable noise with unknown features. The problem of high-order sliding-mode robust differentiator design is to find real-time robust estimations of $\dot{f}_0(t), \ddot{f}_0(t), \dots, f_0^{(n)}(t)$ being exact when $n(t) = 0$. An HOSMRD proposed in Levant (2003) takes on the following form.

$$\begin{aligned} \dot{z}_0 &= v_0 \\ v_0 &= -\lambda_0 |z_0 - f(t)|^{n/(n+1)} \text{sign}(z_0 - f(t)) + z_1 \\ \dot{z}_1 &= v_1 \\ v_1 &= -\lambda_1 |z_1 - v_0|^{(n-1)/n} \text{sign}(z_1 - v_0) + z_2 \\ &\vdots \\ \dot{z}_{n-1} &= v_{n-1} \\ v_{n-1} &= -\lambda_{n-1} |z_{n-1} - v_{n-2}|^{1/2} \text{sign}(z_{n-1} - v_{n-2}) + z_n \\ \dot{z}_n &= -\lambda_n \text{sign}(z_n - v_{n-1}), \end{aligned} \quad (2)$$

where $\lambda_0, \lambda_1, \dots, \lambda_n$ are positive design parameters.

If we let $n = 2$ and $n = 3$, second order and third order sliding mode differentiators can be obtained from (2) respectively, which can provide the estimates for the first and second order derivatives of y .

3.2 Properties of high order sliding mode differentiators

The following two theorems can be derived from the results in Levant (2003).

Theorem 1. Assume that the 3rd order derivative of y has a Lipschitz constant, and there is no measurement noise and all the parameters are chosen properly, then after a finite transient, both the 2nd-order and the 3rd-order sliding mode differentiators can ensure

$$z_0 = y; z_1 = \dot{y}; z_2 = \ddot{y}. \quad (3)$$

Theorem 2. Assume that the 3rd order derivative of y has a Lipschitz constant, and the magnitude of the measurement noises is less than ϵ and all the parameters are chosen properly, then after a finite transient, the 2nd-order sliding mode differentiators can ensure

$$\begin{aligned} |z_1 - \dot{y}| &\leq \mu_{21} \epsilon^{2/3}, \\ |z_2 - \ddot{y}| &\leq \mu_{22} \epsilon^{1/3}, \end{aligned} \quad (4)$$

and the 3rd-order sliding mode differentiators can ensure

$$\begin{aligned} |z_1 - \dot{y}| &\leq \mu_{31} \epsilon^{3/4}, \\ |z_2 - \ddot{y}| &\leq \mu_{32} \epsilon^{1/2}, \end{aligned} \quad (5)$$

where those μ s are vectors of certain positive constants depending only on the parameters of the differentiator and $|\chi|$ is understood as $(|\chi_1| \ \cdots \ |\chi_n|)^T$.

It is interesting to note the above two high order sliding mode differentiators can be used as observers for (1) because they provide the estimate for \dot{y} , which is q_2 . However, high order sliding mode differentiators act more than observers because they provide high order derivatives of y as well.

When measurement noises are present and ϵ is small, it is very interesting to note that the 3rd-order sliding mode differentiators may provide a more accurate estimate of \ddot{y} and \dot{y} than the 2nd-order sliding mode differentiators. However, 2nd-order sliding mode differentiators do not require $f_0^{(3)}(t)$ to exist and be bounded as 3rd-order sliding

mode differentiators do. Therefore, at situations where $f_0(t)$ is smooth enough, it is expected the 3rd-order sliding mode differentiators should perform better than the 2nd-order sliding mode differentiators. While at situations where $f_0^{(3)}(t)$ does not exist everywhere but $f_0^{(2)}(t)$ does, the 2nd-order sliding mode differentiators might have a better performance.

4. ACTUATOR FAULT DIAGNOSIS SCHEMES USING HIGH ORDER SLIDING MODE DIFFERENTIATORS

For (1), if q_2 and \dot{q}_2 were measured, then, based on assumption A2, u could be obtained as

$$u = (g^T(q_1, q_2)g(q_1, q_2))^{-1}g^T(q_1, q_2)[\dot{q}_2 - f(q_1, q_2)] \quad (6)$$

Because q_2 and \dot{q}_2 are not measured, they have to be estimated if one wants to use (6). Note that $q_2 = \dot{y}$ and $\dot{q}_2 = \ddot{y}$, both the 2nd-order and the 3rd-order sliding mode differentiators presented in the previous section can be used to estimate q_2 and \dot{q}_2 . In this way, u can be estimated as

$$\hat{u} = (g^T(q_1, z_1)g(q_1, z_1))^{-1}g^T(q_1, z_1)[z_2 - f(q_1, z_1)] \quad (7)$$

Denote the ideal control as u^* , which can always be computed. When there is no actuator fault, $u = u^*$. However, when actuator faults are in presence, $u \neq u^*$. Based on this observation and using (7), the following residuals are defined

$$r_j = |\hat{u}_j - u_j^*|, j = 1, 2, \dots, m. \quad (8)$$

In noise free situation, because high order sliding mode differentiators are exact, one has $\hat{u} = u$ after the transient period. If there is no actuator fault, one will have $r_j = 0$ for all $j = 1, 2, \dots, m$. Similarly, if the magnitude of the measurement noise is small, r_j for all $j = 1, 2, \dots, m$ should also be small.

Based on the above discussions, two actuator fault diagnosis schemes using the 2nd order (3rd order) sliding mode differentiators given by (2) are presented as follows.

- (1) Using the 2nd order (3rd order) sliding mode differentiators given by (2) to obtain z_1 and z_2 as the estimate of \dot{y} and \ddot{y} .
- (2) Compute u^* according to controller design.
- (3) For each $j = 1, 2, \dots, m$, compute $r_j = |\hat{u}_j - u_j^*|$.
- (4) Choose a threshold $\epsilon_{Thre,j}$ for each $|r_j(t)|$.
- (5) For each $1 \leq j \leq m$, compare the residual $|r_j(t)|$ with the threshold $\epsilon_{Thre,j}$. If any residual goes beyond its corresponding threshold, faults are detected.
- (6) Count the number of residuals that exceed their thresholds, and it is the number of actuator faults. The faulty actuators are isolated as actuators corresponding to those residuals exceeding their thresholds.

Because measurement noises and other unconsidered uncertainties may exist, $\epsilon_{Thre,j}$ should be chosen not too small. On the other hand, too large $\epsilon_{Thre,j}$ may increase the missed detections. Trade-off has to be made on the choice of a suitable threshold.



Fig. 1. 3D Crane provided by the InTeCo Ltd

Remark 1. The only difference in the two fault diagnosis schemes is that different high order sliding mode differentiators are used. The reason for using two different high order sliding mode differentiators is to compare their effects in derivative estimation and in fault diagnosis as well.

5. APPLICATIONS TO A LABORATORY 3D CRANE: SIMULATIONS AND EXPERIMENTS

In this section, a brief introduction of a laboratory 3D Crane and its nonlinear mathematical model is first presented. Then, some simulations are carried out to show the efficacy of the proposed actuator fault diagnosis schemes. Finally, some experiments are provided to test the effect of the 3rd order scheme in practical systems.

5.1 A laboratory 3D Crane and its nonlinear mathematical model

The experimental setup of the 3D Crane provided by the InTeCo Ltd is shown in Figure 1.

It consists of a rail moving along the frame, a cart moving on the rail, and a payload being shifted up and down. The system has three control inputs.

The crane model used for simulations is the 3D Crane simulation model provided by the InTeCo Ltd, which takes the following form

$$\begin{aligned} \dot{q}_1 &= q_2 \\ \dot{q}_2 &= f(q_1, q_2) + g(q_1, q_2)u \\ y &= q_1 \end{aligned} \quad (9)$$

where $q_1 = (x_1 \ x_3 \ x_5 \ x_7 \ x_9)^T$, $q_2 = (x_2 \ x_4 \ x_6 \ x_8 \ x_{10})^T$, x_1 is the distance of the cart from the center of the rail, x_3 is the distance of the rail with the cart from the center of the construction frame, x_5 is the acute angle between the lift-line of the payload and the rail, x_7 is the acute angle between the lift-line of the payload and the vertical line, and finally x_9 is the length of the lift-line. $u = (u_1 \ u_2 \ u_3)^T$ with u_1 , u_2 , and u_3 being control components along the directions related to x_1 , x_3 , and x_9 .

$f(q_1, q_2) = (f_1 \ f_2 \ f_3 \ f_4 \ f_5)^T$ and $g(q_1, q_2) = (g_{ij})_{5 \times 3}$ are given as follows

$$\begin{aligned} f_1 &= -T_1 x_2 - T_{sy} \text{sign}(x_2) \\ &\quad - \mu_1 \cos(x_5) (-T_3 x_{10} - T_{sz} \text{sign}(x_{10})), \end{aligned}$$

$$\begin{aligned}
f_2 &= -T_2x_4 - T_{sx} \text{sign}(x_4) \\
&\quad - \mu_2 \sin(x_5) \sin(x_7) (-T_3x_{10} - T_{sz} \text{sign}(x_{10})), \\
f_3 &= -(T_1x_2 + T_{sy} \text{sign}(x_2)) \sin(x_5) / x_9 \\
&\quad + (\sin(x_5) \cos(x_5) x_8^2 x_9 / x_9 + g \cos(x_5) \cos(x_7)) / x_9 \\
&\quad + \frac{\mu_2 \sin(x_5) \cos(x_5) \sin^2(x_7) (-T_3x_{10} - T_{sz} \text{sign}(x_{10}))}{x_9} \\
&\quad + \cos(x_5) \sin(x_7) (T_2x_4 + T_{sx} \text{sign}(x_4)) / x_9 \\
&\quad - \mu_1 \sin(x_5) \cos(x_5) (-T_3x_{10} - T_{sz} \text{sign}(x_{10})) / x_9 \\
&\quad - 2x_6x_{10} / x_9, \\
f_4 &= -(g \sin(x_7) + 2x_6x_8x_9 \cos(x_5)) / (x_9 \sin(x_5)) \\
&\quad + \frac{\mu_2 \sin(x_5) \sin(x_7) \cos(x_7) (-T_3x_{10} - T_{sz} \text{sign}(x_{10}))}{x_9 \sin(x_5)} \\
&\quad - 2x_8x_{10} \sin(x_5) / (x_9 \sin(x_5)) \\
&\quad + \cos(x_7) (T_2x_4 + T_{sx} \text{sign}(x_4)) / (x_9 \sin(x_5)), \\
f_5 &= \cos(x_5) (T_1x_2 + T_{sy} \text{sign}(x_2)) \\
&\quad + x_8^2 x_9 \sin^2(x_5) + g \sin(x_5) \cos(x_7) \\
&\quad + \mu_2 \sin^2(x_5) \sin^2(x_7) (-T_3x_{10} - T_{sz} \text{sign}(x_{10})) \\
&\quad + \sin(x_5) \sin(x_7) (T_2x_4 + T_{sx} \text{sign}(x_4)) \\
&\quad + \mu_1 (-T_3x_{10} - T_{sz} \text{sign}(x_{10})) \\
&\quad - \mu_1 \sin^2(x_5) (-T_3x_{10} - T_{sz} \text{sign}(x_{10})) \\
&\quad + x_6^2 x_9 - T_3x_{10} - T_{sz} \text{sign}(x_{10}), \tag{10}
\end{aligned}$$

$$\begin{aligned}
g_{11} &= k_1, g_{12} = 0, g_{13} = k_3 \mu_1 \cos(x_5), \\
g_{21} &= 0, g_{22} = k_2, g_{23} = k_3 \mu_2 \sin(x_5) \sin(x_7), \\
g_{31} &= k_1 \sin(x_5) / x_9, g_{32} = -k_2 \cos(x_5) \sin(x_7) / x_9, \\
g_{33} &= k_3 \frac{-\mu_2 \sin(x_5) \cos(x_5) \sin^2(x_7) + \mu_1 \sin(x_5) \cos(x_5)}{x_9}, \\
g_{41} &= 0, g_{42} = -k_2 \cos(x_7) / (x_9 \sin(x_5)), \\
g_{43} &= -k_3 \mu_2 \sin(x_5) \sin(x_7) \cos(x_7) / (x_9 \sin(x_5)), \\
g_{51} &= -k_1 \cos(x_5), g_{52} = -k_2 \sin(x_5) \sin(x_7), \\
g_{53} &= k_3 (-\mu_2 \sin^2(x_5) \sin^2(x_7) - \mu_1 + \mu_1 \sin^2(x_5) - 1). \tag{11}
\end{aligned}$$

The parameters are

$$\begin{aligned}
\mu_1 &= 0.4156, \mu_2 = 0.1431, \\
k_1 &= 49.8636, k_2 = 16.0336, k_3 = -129.8258, \\
T_1 &= 11.5242, T_2 = 26.3263, T_3 = 217.3535, \\
T_{sy} &= 6.4935, T_{sx} = 1.4903, T_{sz} = 20.8333. \tag{12}
\end{aligned}$$

5.2 Simulation results on 3D Crane model

In all simulations, noises at the level of 10^{-6} are added to the five measured states, and the noisy state measurements are sent directly to the high order sliding mode differentiators to get the needed derivatives. A PID controller is used to control the system outputs x_1, x_3, x_9 to track three reference outputs: $y_{r1}(t) = 0.2 + 0.1 \sin(0.1\pi t)$, $y_{r2}(t) = 0.15 + 0.15 \sin(0.1\pi t)$, $y_{r3}(t) = 0.2 + 0.1 \sin(0.1\pi t)$, respectively. The λ parameters are chosen as $\lambda_0 = 10, \lambda_1 = 20, \lambda_2 = 30, \lambda_3 = 40$. The sampling period is 0.002.

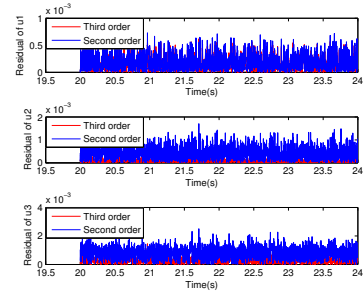


Fig. 2. Input estimation performance comparison of 2nd and 3rd order sliding mode differentiators: no filter case

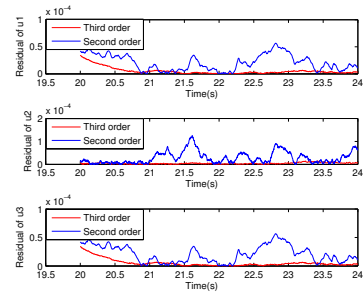


Fig. 3. Input estimation performance comparison of 2nd and 3rd order sliding mode differentiators: filtered case

The performance of 2nd and 3rd order sliding mode differentiators in terms of input estimation error is presented in Fig. 2. The figure shows that 3rd order sliding mode differentiators provided a better input estimation on the time interval where the system outputs are smooth.

Since the input estimation errors provided by both 2nd and 3rd order sliding mode differentiators in Fig. 2 are very noisy, it is filtered in the remaining simulations and in all experiments. After filtering the input estimation errors, the performance of 2nd and 3rd order sliding mode differentiators is given in Fig. 3, where a clearly better performance of 3rd order sliding mode differentiators can be observed.

Because the system model involves sign functions, for the chosen reference outputs, the outputs are not smooth enough to have third order derivatives everywhere. Around those time constants where third order derivatives do not exist, a comparison is also carried out and is shown in Fig. 4, where 2nd order sliding mode differentiators clearly outperform 3rd order sliding mode differentiators.

In terms of fault diagnosis, both schemes using 2nd and 3rd order sliding mode differentiators are tested. Two actuator faults both occurred at 50s are simulated, where the first actuator is stuck at a constant, that is, $u_1 = 0$ after $t > 50s$, and the third one has a loss of effectiveness fault, that is, $u_3(t) = 0.5u_3^*(t)$ after $t > 50s$.

The fault detection and isolation results using both schemes are presented in Figure 5 to Figure 6.

The residuals are chosen according to the normal input estimation behaviors, and the first and third residuals have to be chosen relatively large (0.1, 0.15 respectively)

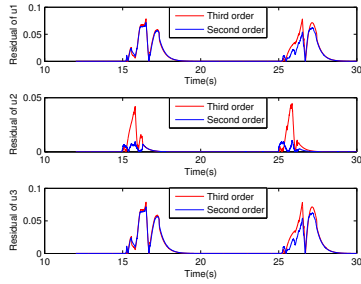


Fig. 4. Input estimation performance comparison of 2nd and 3rd order sliding mode differentiators: no third order derivative case

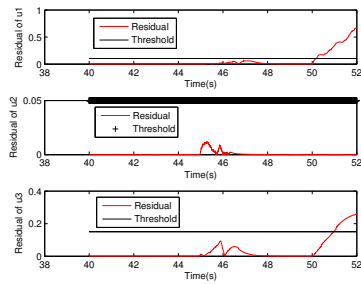


Fig. 5. Actuator fault detection and isolation: the scheme using 2nd order sliding mode differentiators

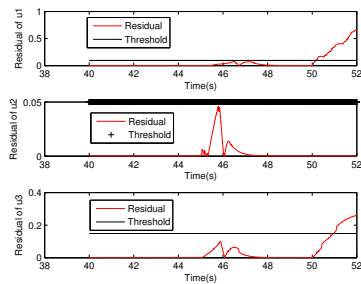


Fig. 6. Actuator fault detection and isolation: the scheme using 3rd order sliding mode differentiators

because of the existence of the sign functions in the system model. In both Figure 5 to Figure 6, it can be seen that faults are detected because in each figure, two residuals exceed their thresholds. Actually, for the scheme using 2nd order sliding mode differentiators, the two actuator faults are detected within $0.162s$ and $0.974s$ respectively. While for the scheme using using 3rd order sliding mode differentiators, the two actuator faults are detected within $0.182s$ and $0.968s$ respectively. Correct isolation decision can be made within one second after the occurrence of faults, that is, the first and the third actuators are faulty, while the second one is normal. In fact, we have found in simulations that, if we let $Tsy = Tsx = Tsz = 0$, the thresholds can be chosen very small at the level of 0.001 , see Fig. 3 for reference.

5.3 Experimental results on 3D Crane

In order to show the applicability of the proposed fault diagnosis schemes to real physical 3D Crane systems, they are further tested through experiments. All the experi-

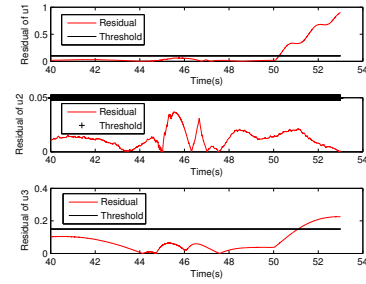


Fig. 7. Experimental results for actuator fault detection and isolation: the scheme using 2nd order sliding mode differentiators

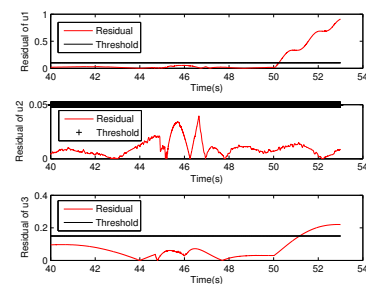


Fig. 8. Experimental results for actuator fault detection and isolation: the scheme using 3rd order sliding mode differentiators

ments are carried out under the same conditions as those in the simulations. For the actuator faults described in the last subsection, the experimental results are presented in Figure 7 and Figure 8, respectively.

It can be seen from Figure 7 and Figure 8 that the two actuator faults can be detected successfully by both schemes because two residuals exceed their thresholds. Actually, for the scheme using 2nd order sliding mode differentiators, the two actuator faults are detected within $0.246s$ and $1.1s$ respectively. While for the scheme using using 3rd order sliding mode differentiators, the two actuator faults are detected within $0.236s$ and $1.168s$ respectively. Correct isolation decision can be made within one and a half second after the occurrence of faults, that is, the first and the third actuators are faulty, while the second one is normal. Compared with the simulation results presented in Figure 5 to Figure 6, the experimental results are very close to those simulation results although input estimation performance is a little bit different and fault detection and isolation time is a little bit longer.

6. CONCLUSIONS

Two actuator fault diagnosis schemes were proposed using 2nd and 3rd order sliding mode differentiators for a class of nonlinear systems with relative degrees higher than one, whose fault diagnosis problems could be very difficult. The proposed schemes were tested through simulations and experiments on the 3D Crane model and the real 3D Crane system offered by the InTeCo Ltd. It is found that experimental results agreed with simulation results very well. Both simulation and experimental results demonstrate the proposed schemes were able to work satisfactorily. It was

observed that, at situations where $f_0(t)$ is smooth enough, the 3rd-order sliding mode differentiators performed better than the 2nd-order sliding mode differentiators, while at situations where the third order derivatives do not exist everywhere but the second order derivatives do, the 2nd-order sliding mode differentiators had a better performance.

REFERENCES

- M. Saif and Y. Guan. A new approach to robust fault detection and identification. *IEEE Trans. on Aerospace and Electronic Systems*, 29: 685-695, 1993.
- Jie Chen, R.J. Patton and Hong-Yue Zhang. Design of unknown input observer and robust fault detection filters. *International Journal of Control*, 63: 85-105, 1996.
- Y. Xiong and M. Saif. A novel design for robust fault diagnostic observers. *Proceedings of the CDC*, pages 592-597. Tampa, Florida, 1998.
- R. Sreedhar, B. Fernandez, and G.Y. Masada. Robust fault detection in nonlinear systems using sliding mode observers. *Proceedings of IEEE CCA*, pages 715-721. Vancouver, BC, Canada, 1993.
- H. Yang and M. Saif. Nonlinear adaptive observer design for fault detection. *Proceedings of the ACC*, pages 1136-1139. Seattle, 1995.
- C. Edwards, S.K. Spurgeon, and R.J. Patton. Sliding mode observers for fault detection and isolation. *Automatica*, 36: 541-553, 2000.
- Y. Xiong and M. Saif. Robust and nonlinear fault diagnosis using sliding mode observers. *Proceedings of the CDC*, pages 567-572. Orlando, Florida, 2001.
- Chee Pin Tan and C. Edwards. Sliding mode observers for reconstruction of simultaneously actuator and sensor faults. *Proceedings of the CDC*, pages 1455-1460. Maui, Hawaii, 2003.
- B. Jiang, M. Staroswiecki and V. Cocquempot. Fault estimation in nonlinear uncertain systems using robust/sliding-mode observers. *IEE Proceedings-Control Theory Appl.*, 151: 29-37, 2004.
- T. Floquet, J. P. Barbot, W. Perruquetti and M. Djemai. On the robust fault detection via a sliding mode observer. *International Journal of Control*, 77: 622-629, 2004.
- W. Chen, and M. Saif. Actuator fault isolation and estimation for uncertain nonlinear systems. *Proceedings of IEEE SMC*, pages 2560-2565. Hawaii, 2005.
- B. Jiang, M. Staroswiecki, and V. Cocquempot. Fault diagnosis based on adaptive observer for a class of nonlinear systems with unknown parameters. *International Journal of Control*, 77: 415-426, 2004.
- H. Yang and M. Saif. State observation, failure detection and isolation(FDI) in bilinear systems. *International Journal of Control*, 67: 901-920, 1997.
- E.E. Yaz and A. Azemi. Actuator fault detection and isolation in nonlinear systems using LMI's and LME's. *Proceedings of the ACC*, pages 1590-1594. Pennsylvania, 1998.
- R. Rajamani and A. Ganguli. Sensor fault diagnosis for a class of nonlinear systems using linear matrix inequalities. *International Journal of Control*, 77: 920-930, 2004.
- W. Chen and M. Saif. Unknown Input Observer Design for a Class of Nonlinear Systems: an LMI Approach. *Proceedings of the ACC*, pages 834 - 838. Minneapolis, Minnesota, 2006.
- R. Seliger and P.M. Frank. Fault diagnosis by disturbance decoupled nonlinear observers. *Proceedings of the CDC*, pages 2248-2253. Brighton, England, 1991.
- R. Seliger and P.M. Frank. Robust component fault detection and isolation in nonlinear dynamic systems using nonlinear unknown input observers. *Proceedings of the IFAC/IMACS Symposium SAFEPROCESS'91*, pages 313-318, Baden-Baden, Germany, 1991.
- H. Hammouri, M. Kinnaert, and E. H. El Yaagoubi. Observer-Based approach to fault detection and isolation for nonlinear systems. *IEEE Trans. on Automatic Control*, 44: 1879-1884, 1999.
- C.D. Persis and A. Isidori. A geometric approach to nonlinear fault detection and isolation. *IEEE Trans. on Automatic Control*, 46: 853-865, 2001.
- C. Join, J.-C. Ponsart, D. Sauter and D. Theilliol. Nonlinear filter design for fault diagnosis: application to the three-tank systems. *IEE Proceedings-Control Theory Appl.*, 152: 55-64, 2005.
- A. Levant. Higher-order sliding modes, differentiation and output-feedback control. *International Journal of Control*, 76: 924-941, 2003.
- T. Floquet and J.P. Barbot. A sliding mode approach of unknown input observers for linear systems. *Proceedings of the CDC*, pages 1724-1729. Bahamas, 2004.
- J. Davila, L. Fridman, A. Levant. Second-order sliding mode observer for mechanical systems. *IEEE Transactions on Automatic Control* 50: 1785-1789, 2005.
- N.K. Msirdi, A. Rabhi, L. Fridman, J. Davila, and Y. Delanne. Second order sliding mode observer for estimation of velocities, wheel sleep, radius and stiffness. *Proceedings of the ACC*, pages 3316-3321. Minneapolis, Minnesota, 2006.
- W. Chen and M. Saif. High-order sliding-mode differentiator based actuator fault diagnosis for linear systems with arbitrary relative degree and unmatched Unknown Inputs. *Proceedings of the CDC*, pages 1153-1158. San Diego, CA, 2006.
- W. Chen and M. Saif. Actuator fault diagnosis for uncertain linear systems using a high order sliding mode robust differentiator (HOSMRD). *International Journal of Robust and Nonlinear Control*, to appear.
- W. Chen and M. Saif. Actuator fault diagnosis in affine nonlinear systems with unknown inputs. *Proceedings of the CDC'07*, accepted.
- Q. Wu and M. Saif. Robust fault detection and diagnosis for a multiple satellite formation flying system using second order sliding mode and wavelet network. *Proceedings of the ACC*, pages 426-431. New York, 2007.
- C. Edwards, L. Fridman, and M. L. Thein. Fault reconstruction in leader/follower spacecraft system using high order sliding mode observers. *Proceedings of the ACC*, pages 408-413. New York, 2007.